Propensity rules for excitation of atoms in high-lying doubly excited states by charged-particle impact

Tohru Atsumi* and Tokuichi Ishihara
Department of Applied Physics and Chemistry, The University of Electro-Communications, Chofu-shi, Tokyo, 182 Japan

Naoto Koyama
Division of Affairs of Foreign Students, The University of Electro-Communications, Chofu-shi, Tokyo, 182 Japan

Michio Matsuzawa
Department of Applied Physics and Chemistry, The University of Electro-Communications, Chofu-shi, Tokyo, 182 Japan†
and Institute for Molecular Science, Myodaiji, Okazaki, 444 Japan
(Received 6 July 1990)

For the $^1P^o$-$^1S^e$, $^1P^o$-$^1D^e$, $^1D^e$-$^1S^e$, and $^1D^e$-$^1P^o$ double-electron excitation processes of He in high-lying doubly excited states by charged-particle impact, we have evaluated the Born cross sections using the hyperspherical wave functions. Together with our previous results [Motoyama, Koyoma, and Matsuzawa, Phys. Rev. A **38**, 670 (1988); Matsuzawa, Atsumi, and Koyama, *ibid.* **41**, 3596 (1990)], we have theoretically found a set of propensity rules for these excitation processes between the doubly excited states with $L \leq 2$. These rules indicate that a He atom in a strongly correlated doubly excited state tends to conserve its internal state as a flexible e-He^{2+}-e linear triatomic molecule during the excitation processes except for the restriction arising from the Pauli exclusion principle. How the exclusion principle modifies the above-mentioned propensity rules for singlet-singlet optically allowed excitation processes depends on the radial correlation of the initial state. The behaviors of the doubly excited atoms in rotationally and/or vibrationally excited states as the flexible linear triatomic molecule tend to deviate from those predicted by the propensity rules so obtained. This is due to the fact that there are no final states available for the propensity rules to specify because of the restriction arising from the cutoff of the quantum numbers.

I. INTRODUCTION

In our previous papers[1-3] we made a theoretical investigation of the collisional properties of He atoms in high-lying doubly excited states, i.e., in $^1S^e$-$^1S^e$, $^1S^e$-$^1P^o$, $^1S^e$-$^1D^e$, $^1P^o$-$^1P^o$, and $^1D^e$-$^1D^e$ electron-impact excitation processes. So far, we have tried to understand how an atom in a doubly excited state behaves when it interacts with charged particles perturbatively. Namely, our research interest lies in understanding the correlation effects in collision dynamics. Therefore, we focused our theoretical studies on excitation processes between the intrashell high-lying doubly excited states in which the correlated motion of two atomic electrons play a decisive role. In order to do this, we employed the hyperspherical coordinate approach[4] to generate the wave functions of the doubly excited states and to calculate their energy levels.[5-7] We evaluated the Born excitation cross sections and found some systematic trends, i.e., propensity rules in collision dynamics involving the doubly excited atoms. To interpret these propensity rules obtained, we relied on the rovibrator model of the doubly excited states proposed by Herrick and Kellman[8,9] and the classification scheme of the doubly excited states proposed by Lin.[4]

Here we extend our theoretical studies to $^1P^o$-$^1S^e$, $^1P^o$-$^1D^e$, $^1D^e$-$^1S^e$, and $^1D^e$-$^1P^o$ electron-impact excitation processes, i.e.,

$$e + \mathrm{He}^{**}(i) \rightarrow e + \mathrm{He}^{**}(f) , \tag{1}$$

where i (f) denotes the initial (final) doubly excited states of He. Furthermore, we can expect that the propensity rules obtained here also apply to excitation processes of doubly excited atoms by charged particles other than electrons in the energy regions where Born approximation is valid. To confirm it, we investigate excitation processes by C^{6+} ion impact, i.e.,

$$C^{6+} + \mathrm{He}^{**}(i) \rightarrow C^{6+} + \mathrm{He}^{**}(f) . \tag{2}$$

We also analyze how the angular-momentum transfer occurs from relative motion to the excited atoms in the $^1P^o$-$^1P^o$, $^1P^o$-$^1D^e$, $^1D^e$-$^1P^o$, and $^1D^e$-$^1D^e$ excitation processes. We summarize the propensity rules obtained so far in excitation of He atoms in high-lying doubly excited states with $L \leq 2$ by charged-particle impact using the rovibrator model together with the previous results.[1-3] Finally we translate the propensity rules based on the rovibrator model into those based on the molecular-orbital (MO) model for the doubly excited states proposed by Feagin and Briggs,[10,11] and discuss their physical interpretation.

II. CLASSIFICATION SCHEMES OF DOUBLY EXCITED STATES

To discuss collision dynamics involving the doubly excited states, we employ two classification schemes based on the rovibrator model[4,8,9] and the MO model recently proposed.[10,11] Here we give a brief description of these models, since we will refer to them in a later discussion.

In order to label the energy levels of strongly correlated doubly excited states, Lin[4,12] proposed the classification scheme, i.e., to employ a set of quantum numbers, $[N(K,T)^A n]^{2S+1}L^{\pi}$. Here, N ($\leq n$) is the principal quantum number of an inner (outer) electron and K, T, and A are the so-called correlation quantum numbers. Other quantum numbers L, S, and π are defined as usual. The quantum numbers K and T originate from the group-theoretic approach by Herrick and Sinanoglu,[13] and describe angular correlation. The quantum number K is a measure of $\langle -\mathbf{r}_< \cdot \hat{\mathbf{r}}_> \rangle$, i.e., the projection of the inner electron radius vector onto that of the outer electron, while T^2 is proportional to $\langle (\mathbf{L}\cdot\hat{\mathbf{r}}_>)^2 \rangle$. These quantum numbers take the following values:[13]

$$T=0,1,2,\ldots,\min(L,N-1)\ , \tag{3}$$

$$K=N-T-1,N-T-3,\ldots,-(N-T-1)\ . \tag{4}$$

The quantum number A introduced by Lin[12] describes the radial correlation at the finite hyperradius $R=(r_1^2+r_2^2)^{1/2}$. This quantum number is set equal to $+$ ($-$) if an angular channel function has an antinode (node) at the potential ridge, i.e., $\alpha=\pi/4$, where α is the hyperangle defined by $\alpha=\tan^{-1}(r_2/r_1)$. Other channels are assigned to $A=0$, where their channel functions do not have substantial amplitude at $\alpha=\pi/4$ for almost all R but reside away at $\alpha=0$ or $\pi/2$. Watanabe and Lin[14] made a more detailed quantitative analysis of the set of the correlation quantum numbers $(K,T)^A$ using the body-fixed frame attached to the atoms and identified the following relation:

$$A=\begin{cases}\pi(-1)^{S+T}=\pi(-1)^{S+N-K+1}, & K>L-N\\ 0, & K\leq L-N.\end{cases} \tag{5}$$

This relation arises from the fact that two atomic electrons obey Fermi statistics. For all states with $L\geq 2N-1$, A is set equal to zero for all channels. These states with $A=0$ are considered to be singly excited states. According to the collective rovibrational interpretation of the supermultiplet structure of the doubly excited states,[9,10] v ($=N-K-1$) corresponds to the quantum number of the doubly degenerate bending vibrational modes of the flexible ("floppy") e-He^{2+}-e linear triatomic molecule, while T is the vibrational angular momentum around the mean molecular axis. Furthermore, it is quite useful to introduce the radial bending quantum number $n_2=(v-T)/2$, i.e., the number of nodes in the vibrational motion in θ_{12}, i.e., the angle between the two radius vectors of two electrons on the body-fixed frame. Finally the number of the nodes in the hyperradial motion within each channel is given by $n-n_{\min}$, where $n_{\min}$ is the lowest n given by the following relation, i.e.,

$$n_{\min}=\begin{cases}N & \text{for } A=+\\ N+1 & \text{for } A=-\\ N+1 & \text{for } A=0.\end{cases} \tag{6}$$

However, for successive higher channels with $A=0$, n increases by one unit for each $\Delta K=-1$ instead of Eq. (4). Here it should be noted that all the quantum numbers such as K, T, A, v, and n_2 are approximately conserved because the two-electron-atom Schrödinger equation is only approximately separable into the collective modes of the e-He^{2+}-e linear triatomic molecule in the case where electron correlation plays an essential role.

Recently Feagin and Briggs[10,11,15,16] developed the molecular-orbital method to treat correlated motion of two-atomic electrons. In this model, the individual motion of the two electrons with respect to the nucleus is considered to be approximately separable into two modes of two-electron motions. The first is the vibrational motion of the interelectronic coordinate $\mathbf{R}=\mathbf{r}_1-\mathbf{r}_2$ with the reduced mass of the two electrons where $\mathbf{r}_1$ and $\mathbf{r}_2$ are the radius vectors of two electrons with respect to the nucleus. The latter is the motion of the center of mass with respect to the nucleus. This motion is described by the coordinate $\mathbf{r}=(\mathbf{r}_1+\mathbf{r}_2)/2$ of the center of mass of the electron pair with respect to the nucleus, where $\mathbf{R}$ and $\mathbf{r}$ are a set of Jacobi coordinates of three-particle system, i.e., two electrons and the nucleus. This center-of-mass motion is approximately separable and described by the MO method well known for the hydrogen molecular ion H_2^+.

The MO's are characterized by the quantum numbers T, t, n_λ, and n_μ. Here T is the projection of the total angular momentum L onto the interelectronic axis along $\mathbf{R}$, the σ,π,δ quantum numbers in the "dielectronic" MO. There is the gerade-ungerade symmetry of the dielectronic MO. This symmetry is specified by quantum number t if one sets $t=1$ for g symmetry and $t=-1$ for u symmetry. The quantum numbers n_λ and n_μ are the MO quantum numbers corresponding to the spheroidal coordinates $\lambda=(r_1+r_2)/R$ and $\mu=(r_1-r_2)/R$.

Feagin and Briggs[11] discussed the correspondence between the sets of the quantum numbers of the two models. The quantum number T is the same as the vibrational angular momentum T previously defined in the rovibrator model. For other quantum numbers, they identified the following relations, i.e.,

$$K=n_1-n_2=[n_\mu/2]-n_\lambda\ , \tag{7}$$

$$A=(-1)^{n_\mu}\ , \tag{8}$$

$$\pi(-1)^S=(-1)^t\ , \tag{9}$$

where n_1 and n_2 are the parabolic quantum numbers of the separated-atom limit, to which the MO correlates and the symbol $[x]$ denotes the largest integer less than x.

In the following, we mainly use the rovibrator model to describe the collision dynamics as we did in our previous papers[1-3] and translate our results expressed in the rovibrator model into those used in the MO model in Sec. IV, and discuss their physical interpretation.

III. NUMERICAL COMPUTATION AND CALCULATED RESULTS

We have calculated the Born cross sections σ_{if}, i.e.,

$$\sigma_{if}=\frac{4\pi Z^2}{v_i^2}\frac{1}{E_f-E_i}\int_{|k_i-k_f|}^{k_i+k_f}F_{if}(K)\frac{1}{K}dK \ , \tag{10}$$

for excitation processes (1) and (2). Hereafter atomic units ($m_e=e=\hbar=1$) are used unless otherwise stated. Here v_i is the velocity of an incident particle, Z is its charge, k_i (k_f) is the wave number of an incident (scattered) particle, and E_i (E_f) is the energy of the initial (final) doubly excited state. The symbol $F_{if}(K)$ denotes the generalized oscillator strength (GOS) between the doubly excited states defined by

$$F_{if}(K)=\frac{2(E_f-E_i)}{K^2}\langle|\varepsilon_{if}(\mathbf{K})|^2\rangle \ , \tag{11}$$

where $\mathbf{K}$ is the momentum transfer and $\varepsilon_{if}(\mathbf{K})$ is the transition form factor

$$\varepsilon_{if}(\mathbf{K})=\left\langle f\left|\sum_{j=1}^{2}\exp(i\mathbf{K}\cdot\mathbf{r}_j)\right|i\right\rangle \ . \tag{12}$$

Here the large angular brackets in Eq. (12) mean that the squared transition form factors are averaged over the initial magnetic substates and summed over the final magnetic ones. We have adopted the same procedures as those employed in our previous papers.[1-3] Namely, we have assumed that the coupling of these doubly excited states to continua associated with excited states of He^+ can be neglected and that the collisional excitation processes between the quasibound doubly excited states are well defined for collision processes (1) and (2), as was done in our previous papers.[1-3] We have used the hyperspherical wave functions for high-lying doubly excited states to calculate the GOS between the doubly excited states. The $^1S^e$ channel functions are expanded over a set of 49 basis functions, while 64 and 95 basis functions have been used for $^1P^o$ and $^1D^e$ states, respectively. Here the numbers of the basis functions have been fixed after the convergence of our calculated results for the energy levels was carefully tested.[5]

We have evaluated the Born cross sections for $^1P^o$-$^1D^e$, $^1D^e$-$^1P^o$, $^1P^o$-$^1S^e$, and $^1D^e$-$^1S^e$ excitation processes for collision processes (1). In Fig. 1 we give some typical examples of the calculated cross sections for $^1P^o$-$^1D^e$ excitation processes from the initial states with $A=+$ and $-$. These figures show quite simple, i.e., monotonically decreasing energy dependence for almost all the cross sections. Therefore, we adopt the value of the Born cross sections at fixed energy, i.e., 50 eV as the measure of the likelihood of each excitation processes as we did in our previous paper.[3] Here the Born approximation remains to be valid at 50 eV incident energy for the doubly excited states studied here, because this incident energy is much larger than the excitation energies between the doubly excited states, i.e., at most $\sim 2-3$ eV.

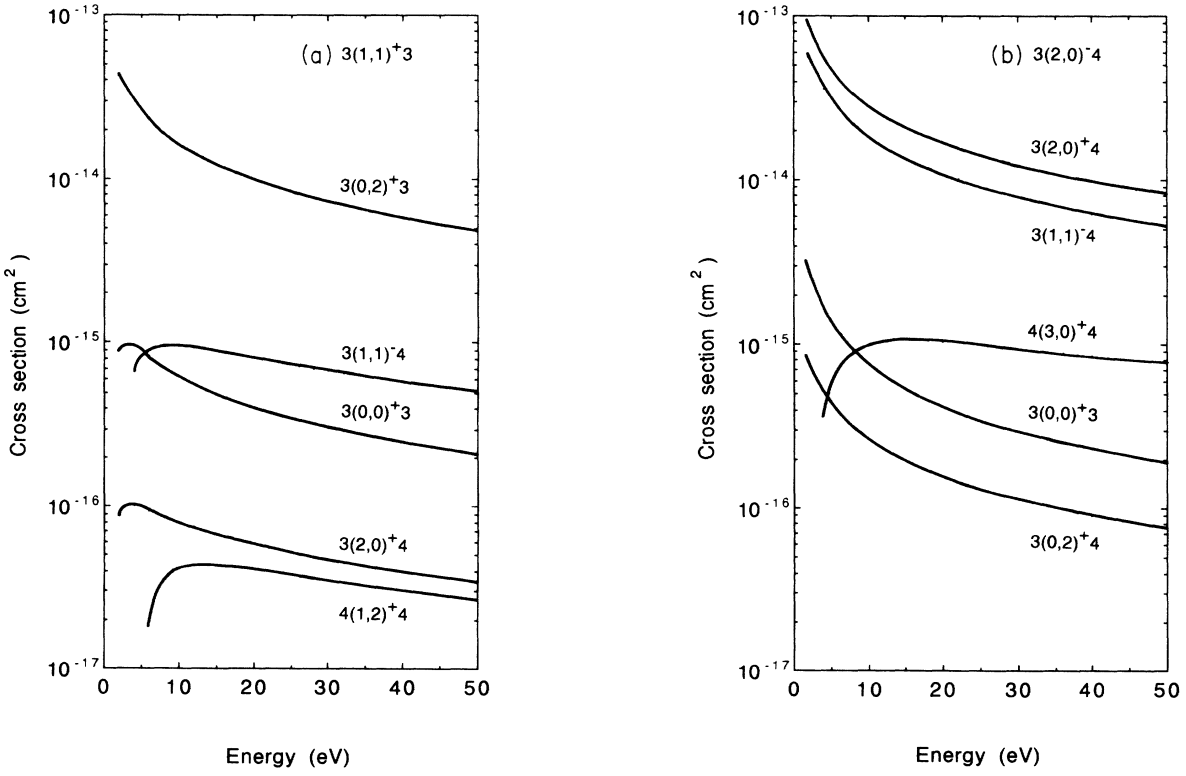

FIG. 1. Born cross sections for the $^1P^o$-$^1D^e$ excitation process of He by electron impact from the following initial states: (a) $[3(1,1)^+3]^1P^o$ and (b) $[3(2,0)^-4]^1P^o$. The labeling attached to each curve specifies the final state.

TABLE I. Born cross sections for the $^1P^o$-$^1D^e$ excitation processes of He by electron impact at 50 eV incident energy (a) $3(1,1)^+3 \rightarrow N(K,T)^An$ for $N=3$ or 4; (b) $3(2,0)^-4 \rightarrow N(K,T)^An$ for $N=3$ or 4 with the changes of the quantum numbers during excitation processes. The notation $[x]$ denotes 10^x.

Initial states $N(K,T)^An$	Final states $N(K,T)^An$	Cross sections (cm^2)	Change of the quantum numbers ΔN	ΔA	Δv	ΔT	Δn_2	Δn
$3(1,1)^+3$	$3(0,2)^+3$	4.9[−15]	0	0	1	1	0	0
	$3(1,1)^-4$	5.2[−16]	0	×	0	0	0	1
	$3(0,0)^+3$	2.1[−16]	0	0	1	−1	1	0
	$3(2,0)^+4$	3.4[−17]	0	0	−1	−1	0	1
	$4(1,2)^+4$	2.7[−17]	1	0	1	1	0	1
$3(2,0)^-4$	$3(2,0)^+4$	8.2[−15]	0	×	0	0	0	0
	$3(1,1)^-4$	5.3[−15]	0	0	1	1	0	0
	$4(3,0)^+4$	7.7[−16]	1	×	0	0	0	0
	$3(0,0)^+3$	1.9[−16]	0	×	2	0	1	−1
	$3(0,2)^+4$	7.6[−17]	0	×	2	2	0	0

TABLE II. Born cross sections for the $^1D^e$-$^1P^o$ excitation processes of He by electron impact at 50 eV incident energy (a) $3(2,0)^+3 \rightarrow N(K,T)^An$ for $N=3$ or 4; (b) $3(1,1)^-4 \rightarrow N(K,T)^An$ for $N=3$ or 4 with the changes of the quantum numbers during excitation processes. The notation $[x]$ denotes 10^x.

Initial states $N(K,T)^An$	Final states $N(K,T)^An$	Cross sections (cm^2)	Change of the quantum numbers ΔN	ΔA	Δv	ΔT	Δn_2	Δn
$3(2,0)^+3$	$3(1,1)^+3$	1.7[−15]	0	0	1	1	0	0
	$3(2,0)^-4$	2.7[−16]	0	×	0	0	0	1
	$3(-1,1)^+3$	6.3[−18]	0	0	3	1	1	0
	$3(0,0)^-4$	3.1[−18]	0	×	2	0	1	1
	$4(2,1)^+4$	9.6[−19]	1	0	1	1	0	1
$3(1,1)^-4$	$3(1,1)^+4$	7.2[−15]	0	×	0	0	0	0
	$3(0,0)^-4$	5.3[−15]	0	0	1	−1	1	0
	$3(2,0)^-5$	2.6[−16]	0	0	−1	−1	0	1
	$4(2,1)^+4$	1.1[−16]	1	×	0	0	0	0
	$3(-1,1)^+4$	5.6[−17]	0	×	2	0	1	0

TABLE III. Born cross sections for the $^1P^o$-$^1S^e$ excitation processes of He by electron impact at 50 eV incident energy (a) $3(1,1)^+3 \rightarrow N(K,T)^An$ for $N=3$ or 4; (b) $3(2,0)^-4 \rightarrow N(K,T)^An$ for $N=3$ or 4 with the changes of the quantum numbers during excitation processes. The notation $[x]$ denotes 10^x.

Initial states $N(K,T)^An$	Final states $N(K,T)^An$	Cross sections (cm^2)	Change of the quantum numbers ΔN	ΔA	Δv	ΔT	Δn_2	Δn
$3(1,1)^+3$	$3(0,0)^+3$	1.9[−15]	0	0	1	−1	1	0
	$3(2,0)^+4$	3.0[−17]	0	0	−1	−1	0	1
	$4(1,0)^+4$	1.4[−18]	1	0	1	−1	1	1
	$4(3,0)^+4$	1.2[−18]	1	0	−1	−1	0	1
	$4(-1,0)^+4$	6.1[−20]	1	0	3	−1	2	1
$3(2,0)^-4$	$3(2,0)^+4$	4.3[−15]	0	×	0	0	0	0
	$4(3,0)^+4$	1.6[−16]	1	×	0	0	0	0
	$3(0,0)^+4$	5.1[−17]	0	×	2	0	1	0
	$4(1,0)^+4$	3.7[−18]	1	×	2	0	1	0
	$3(-2,0)^+3$	8.6[−19]	0	×	4	0	2	−1

TABLE IV. Born cross sections for the $^1D^e$-$^1S^e$ excitation processes of He by electron impact at 50 eV incident energy (a) $3(2,0)^+3 \rightarrow N(K,T)^A n$ for $N=3$ or 4; (b) $3(1,1)^-4 \rightarrow N(K,T)^A n$ for $N=3$ or 4 with the changes of the quantum numbers during excitation processes. The notation $[x]$ denotes 10^x.

Initial states $N(K,T)^A n$	Final states $N(K,T)^A n$	Cross sections (cm^2)	Change of the quantum numbers ΔN	ΔA	Δv	ΔT	Δn_2	Δn
$3(2,0)^+3$	$3(0,0)^+3$	3.5[−17]	0	0	2	0	1	0
	$3(2,0)^+4$	9.1[−18]	0	0	0	0	0	1
	$4(3,0)^+4$	4.4[−19]	1	0	0	0	0	1
	$4(1,0)^+4$	1.1[−19]	1	0	2	0	1	1
	$3(-2,0)^+3$	5.7[−20]	0	0	4	0	2	0
$3(1,1)^-4$	$3(0,0)^+4$	4.6[−17]	0	×	1	−1	1	0
	$3(2,0)^+5$	1.9[−17]	0	×	−1	−1	0	1
	$4(1,0)^+4$	8.5[−18]	1	×	1	−1	1	0
	$3(-2,0)^+3$	8.5[−18]	0	×	3	−1	2	−1
	$4(3,0)^+4$	4.7[−18]	1	×	−1	−1	0	0

Table I shows typical examples of the singlet-singlet optically allowed $^1P^o$-$^1D^e$ excitation cross sections at 50 eV from the intrashell initial states and from the intershell initial states together, with the information on the change of the quantum numbers for the rovibrator model, which occurs during the excitation process. Here we list the change of the quantum number v instead that of K as we did in Ref. 3. This enables us to easily understand the character of the transitions based on the rovibrational interpretation of the collective motion of the two atomic electrons. For the initial states with $A=+$, the processes with $\Delta v=\Delta T=1$ and with all other quantum numbers unchanged are most likely to occur in each manifold. The rovibrator model tells us that a He atom in a doubly excited state of a floppy e-He^{2+}-e linear triatomic molecule tends to be vibrationally excited in the doubly degenerate bending vibrational modes and to be rotationally excited around the mean molecular axis. This systematic trend is quite similar to that seen in the $^1S^e$-$^1P^o$ excitation. For the initial states with $A=-$, the excitation processes with $\Delta A \neq 0$ and with all other quantum numbers unchanged are most likely to take place. Here it should be noted that the $^1S^e$ states have only $A=+$.

Table II indicates that for the singlet-singlet optically allowed $^1D^e$-$^1P^o$ excitation processes, the trends similar to those for the $^1P^o$-$^1D^e$ processes can be seen. Namely, for the initial states with $A=+$, the excitation process with $\Delta v=\Delta T=1$ and with all other quantum numbers unchanged is most likely to occur in each manifold while for the initial state with $A=-$, the excitation process with $\Delta A \neq 0$ and with all other quantum numbers unchanged is most likely to take place.

For the singlet-singlet optically allowed $^1P^o$-$^1S^e$ excitation processes, Table III indicates that for the initial states with $A=-$, one sees the trends similar to those obtained in other optically allowed $^1P^o$-$^1D^e$ and $^1D^e$-$^1P^o$ excitation processes. However, the initial states with $A=+$ show the trends different from those for the $^1P^o$-$^1D^e$, and $^1D^e$-$^1P^o$ excitation processes, i.e., the excitation process $\Delta v=1, \Delta T=-1, \Delta n_2=1$ with all other quantum numbers unchanged is most likely to occur.

For the optically forbidden $^1D^e$-$^1S^e$ excitation processes, Table IV gives some typical example in which the following transitions are most likely to take place, i.e., (i) $\Delta v=2$ and all other quantum numbers are unchanged for the initial state with $A=+$ and (ii) $\Delta A \neq 0$, $\Delta v=1$, $\Delta T=-1$, $\Delta n_2=1$ and other quantum numbers are unchanged. This behavior is different from that for the $^1S^e$-$^1D^e$ excitation processes.

We have also investigated collision process (2) in the energy region where the Born approximation is valid, for example, at $E=10$ MeV for C^{6+} ions. We have confirmed that excitation of He by heavy-ion impact shows the same systematic trends, i.e., the propensity rules as those found for process (1) with $\Delta L=0,1,2$ [$\Delta L=L_f-L_i$, where L_i (L_f) is the total angular momentum of the initial (final) state].

Here is should be noted that our numerical calculations have been performed using the hyperspherical coordinate approach, i.e., quite independently of the models which we employ in order to interpret the physical meaning of our calculated results.

IV. DISCUSSION AND CONCLUSIONS

In our previous paper[2] we have pointed out that the radial propensity rule $\Delta A=0$ and the angular propensity rules $\Delta v=\Delta T=0$ ($\Delta n_2=0$) hold for the $^1S^e$-$^1S^e$ and $^1S^e$-$^1D^e$ excitation processes involving the doubly excited states. This is interpreted as a result of isomorphism of the surface density plot of the squared hyperspherical channel functions between the initial and final states. This means that the doubly excited atoms tend to keep their internal states, i.e., their shape as the "triatomic linear molecules" in the body-fixed frame the same as that in the initial state. Because of relation (5), the radial and the angular propensity rules are incompatible with one another for the $^1S^e$-$^1P^o$ excitation processes. The radial propensity rule prevails over the angular ones. The latter are modified into $\Delta v=\Delta T=1$, though $\Delta n_2=0$ remain unchanged. In Ref. 3 we have found that the radial propensity rule $\Delta A=0$ and angular propensity rules

$\Delta v=\Delta T=0$ and $\Delta n_2=0$ also apply to the excitation processes with $\Delta L=0$, though only one electron participates in these transitions between the strongly correlated doubly excited states.

Tables I and II for the singlet-singlet excitation processes with $|\Delta L|=1$ show that the same arguments as that for the $^1S^e$-$^1P^o$ excitation processes apply to the $^1P^o$-$^1D^e$ and $^1D^e$-$^1P^o$ excitation processes with the initial states with $A=+$, though one has different propensity rules for the $^1P^o$-$^1S^e$ excitation. For the initial states with $A=-$, we have seen the same trends for the $^1P^o$-$^1D^e$, $^1D^e$-$^1P^o$, and $^1P^o$-$^1S^e$ excitation processes. In the singlet-singlet excitation processes with $|\Delta L|=1$, two types of the propensity rules are incompatible with one another, because of the Pauli exclusion principle for the two atomic electrons [see relation (5)]. However, in the case with $A=-$, the angular propensity rules dominate over the radial propensity rules for the $^1P^o$-$^1D^e$, $^1D^e$-$^1P^o$, and $^1P^o$-$^1S^e$ excitations. In these cases, the latter is modified into $\Delta A\neq 0$. For the $^1D^e$-$^1S^e$ excitation, the systematic trends are quite different from those for $\Delta L=2$. The deviation from the propensity rules for the $^1P^o$-$^1S^e$ and $^1D^e$-$^1S^e$ excitation processes is considered to originate from the fact that there is no final state available which the propensity rules specify because of the cutoff of the quantum numbers K (or v) and T for the $^1S^e$ final state. Here is should be noted that $\Delta n_2=0$ also applies to the cases studied here except for those of the $^1S^e$ final states. Table V summarizes the propensity rules obtained so far together with the physical interpretation based on the rovibrator model. In this table we have excluded some results for the $^1P^o$-$^1S^e$ and $^1D^e$-$^1S^e$ excitation processes because of the strong restriction for the final $^1S^e$ states arising from the cutoff of the quantum numbers K (or v) and T. We stress here that the propensity rule $\Delta n_2=0$ holds for all cases listed in Table V.

In Ref. 3 we investigated double-electron excitation processes for the case of $\Delta L=0$. We found that there is a sharp difference between the propensity rule for the $^1S^e$-$^1S^e$ excitation and that for the $^1P^o$-$^1P^o$ and $^1D^e$-$^1D^e$ excitation. Namely, for the $^1P^o$-$^1P^o$ and $^1D^e$-$^1D^e$ double excitation processes, the rotational and vibrational modes as the floppy linear molecule are more likely to be excited than the stretching mode in the $^1S^e$-$^1S^e$ excitation processes. In order to study this difference, we have made an analysis of the GOS in terms of the components of angular-momentum transfer l from the relative motion to the excited atom. The plane wave is decomposed into the partial waves, i.e.,

$$e^{i\mathbf{K}\cdot\mathbf{r}}=\sum_{l=0}^{\infty}(2l+1)i^l j_l(Kr)P_l(\cos\theta)\ , \tag{13}$$

where θ is the angle between $\mathbf{K}$ and $\mathbf{r}$. Here l can be interpreted to be the angular-momentum transfer from the relative motion to the atom. For example, the $^1P^o$-$^1P^o$ GOS is decomposed into the two components, i.e., $l=0,2$ while the $^1D^e$-$^1D^e$ GOS is decomposed into the three components, i.e., $l=0,2,4$. For both cases, the $l=0$ component mainly contributes to single-electron excitation listed in Table V while the $l=2$ component gives rise to the double-electron excitation with the changes of the angular correlation quantum number K (i.e., v) and T. On the other hand, the $^1S^e$-$^1S^e$ GOS has only the $l=0$ component, which can cause electron-pair excitations only in the stretching mode, because no angular-momentum transfer occurs from the relative motion to the atom. We have also applied this analysis to the $^1P^o$-$^1D^e$ excitation processes where the $^1P^o$-$^1D^e$ GOS is decomposed into the $l=1$ and 3 components. Here we have found that the $l=1$ component mainly gives rise to the electron-pair excitation processes listed in Table V as in the $^1S^e$-$^1P^o$ excitation.

For the double excitation processes with $\Delta L=0$, we

TABLE V. The propensity rules based on the rovibrator model in charged-particle impact excitation of He in the doubly excited states for $|\Delta L|\leq 2$. Some exceptional cases for the $^1P^o$-$^1S^e$ and $^1D^e$-$^1S^e$ excitation processes are excluded because of strong restriction arising from the cutoff of the quantum numbers K and T of the final states.

Transitions	Propensity rules	Interpretation based on the rovibrator model
$\Delta L=0$	$\Delta A=0$ $\Delta v=\Delta T=0$, $\Delta n_2=0$, $\Delta N=0$, $\Delta n=1$	Single electron excitation
$\Delta L=1$ or -1	$A=+$; $\Delta A=0$, $\Delta v=\Delta T=1$, $\Delta n_2=0$, $\Delta N=\Delta n=0$	Bending vibrational excitation and rotational excitation around the molecular axis
	$A=-$; $\Delta A\neq 0$, $\Delta v=\Delta T=0$, $\Delta n_2=0$, $\Delta N=\Delta n=0$	Change of radial correlation
$\Delta L=2$	$\Delta A=0$, $\Delta v=\Delta T=0$, $\Delta n_2=0$, $\Delta N=\Delta n=0$	Rotational excitation as a whole

have seen that the propensity rule $\Delta n_2=0$ holds except for the ${}^1P^o$-${}^1P^o$ and ${}^1D^e$-${}^1D^e$ excitation processes from the initial states with $A=+$.[3] For the ${}^1P^o$-${}^1P^o$ excitation processes we have the propensity rules, $\Delta v=2$, $\Delta T=0$, $\Delta n_2=1$, and all other quantum numbers unchanged. However, in the final ${}^1P^o$ states, there are no states available which can satisfy $\Delta T=2$ because of the cutoff of the quantum number T. Actually for the ${}^1D^e$-${}^1D^e$ excitation, we have found that for the $N=3$ manifold of excitation processes the excitation processes with $\Delta v=2$, $\Delta T=2$, $\Delta n_2=0$, and all other quantum numbers unchanged occur comparable with the excitation processes with $\Delta v=2$, $\Delta T=0$, $\Delta n_2=1$, and all other quantum numbers unchanged though the former is a little less likely to take place than the latter. Furthermore, for the manifold with $N=4$, we have seen that the situation changes, i.e., the former is more likely to occur than the latter. Therefore, we may conclude that the propensity rule $\Delta n_2=0$ also applies to the double-electron excitation processes with $\Delta L=0$ except for the cases where this rule does not hold because of the cutoff of the quantum numbers. Hence, our results are summarized based on the interpretation of the rovibrator model as follows; the radial propensity rule

$$\Delta A=0 , \tag{14}$$

and the angular propensity rules

$$\Delta v=\Delta T=0 \tag{15}$$

hold for the excitation processes of He atoms in the high-lying strongly correlated doubly excited states by charged-particle impact. The latter propensity rules lead to the propensity rule

$$\Delta n_2=0 . \tag{16}$$

The propensity rules (14), (15), and (16) indicate that the doubly excited He atom as the floppy linear triatomic molecule tend to conserve its shape, i.e., its internal state on the body-fixed frame during the excitation processes while it interacts with other charged particles perturbatively. This is interpreted as a result of isomorphism of the charge-density plots of the channel wave functions between the initial excited states and the final ones. This means that there is no change of the nodal structures between the initial- and final-state channel function and guarantees that the overlap of the initial- and final-state wave functions becomes the largest. The behaviors of the doubly excited atoms in "rotationally and/or vibrationally" excited states tend to deviate from the propensity rules in the cases where, in the final channel of collision process (1), there are no final states available that the above propensity rules specify because of the cutoff of the quantum numbers K (or v) and T.

For the singlet-singlet optically allowed excitation with $|\Delta L|=1$, the radial propensity rule is incompatible with the angular ones because the two atomic electrons obey Fermi statistics, i.e., because of the Pauli exclusion principle for two atomic electrons, i.e., relation (5). For the initial states with $A=+$, the angular propensity rules $\Delta v=\Delta T=0$ are modified into

$$\Delta v=\Delta T=1 , \tag{15'}$$

under the condition that the propensity rule (16) remains unchanged. The propensity rule (16) also tends to hold for the double excitation processes with $\Delta L=0$. For the initial states with $A=-$, the angular propensity rules dominate over the radial one. The latter is changed into the propensity rule

$$\Delta A\neq 0 . \tag{14'}$$

The propensity rules (14), (15), and (16), i.e., the concept of the isomorphism with their variants (14') and (15'), give the unified understanding for a wide class of dynamical phenomena involving the doubly excited states. We have also theoretically confirmed that the set of propensity rules (14), (15), and (16) with their variant (15') apply to the excitation of the ground state He as long as the conditions $\Delta N\geq 1$ and $\Delta n\geq 1$ are satisfied.[17] In the threshold excitation of He in the ground state by electron impact,[18] the singlet-triplet transitions are allowed to take place. Therefore, the radial propensity rule (14) and the angular one (15) can coexist with the relation (5). The propensity rules (14), (15), and (16) can explain experimental findings observed in Ref. 18 as was pointed out.[2] Experimental findings on photoabsorption for the double electron excitation of the ground-state helium[19,20] can also be explained by the propensity rules (14), (15'), and (16) as pointed out previously.[4] The concept of the isomorphism can apply to the systematics of the autoionization width, i.e., the partial width is the largest when the continuum channel corresponds to propensity rules (14), (15), (16), and $\Delta N=-1$.[4] Therefore, we conclude that the concept of the isomorphism in the rovibrator model governs a wide class of dynamical phenomena involving the doubly excited states under the conditions that suitable modifications arising from the Pauli exclusion principle are taken into account, if necessary. In other words, the atom in the doubly excited state tends to conserve its internal state as a floppy triatomic linear molecule except for the restriction arising from the Pauli exclusion principle when they interact with other charged particles perturbatively.

Using the correspondence[10,11,15,16] between the rovibrator model and the MO model including relations (7), (8), and (9), we can translate the propensity rules based on the rovibrator model into those based on the MO model. These are written as follows: one has for the radial propensity rule (14)

$$\Delta n_\mu=0 \text{ or even} , \tag{17}$$

and for the angular propensity rules (15),

$$\Delta N=\Delta[n_\mu/2]-\Delta n_\lambda, \quad \Delta T=0 . \tag{18}$$

Here, judging from the overlap between the initial and final wave functions, we may assume that $\Delta n_\mu=0$ is most likely to occur in (17). In this case, one has $\Delta n_\lambda=0$ for $\Delta N=0$. The propensity rule (16), i.e., $\Delta n_2=0$ is translated into

$$\Delta N=\Delta[n_\mu/2]-\Delta n_\lambda+\Delta T . \tag{19}$$

TABLE VI. The propensity rules based on the MO model in charged-particle impact excitation of He in the doubly excited states for $|\Delta L| \leq 2$. The propensity rules $\Delta A = 0$ ($\Delta A \neq 0$) is translated into $\Delta n_\mu = 0$ ($\Delta n_\mu = 1$).

Transitions	Propensity rules	Expressions for $\Delta T = 0$ or 1 in the conventional MO quantum numbers
$\Delta L = 0$	$\Delta n_\lambda = 0$, $\Delta n_\mu = 0$ $\Delta T = 0$, $\Delta N = 0$, $\Delta n = 1$	$^1S^e$-$^1S^e$; $\sigma_g \rightarrow \sigma_g$ $^1P^o$-$^1P^o$; $\sigma_u \rightarrow \sigma_u$, $\pi_u \rightarrow \pi_u$ $^1D^e$-$^1D^e$; $\sigma_g \rightarrow \sigma_g$, $\pi_g \rightarrow \pi_g$, $\delta_g \rightarrow \delta_g$
$\Delta L = 1$ or -1	n_μ = even; $\Delta n_\lambda = 1$, $\Delta n_\mu = 0$, $\Delta T = 1$, $\Delta N = \Delta n = 0$	$^1S^e$-$^1P^o$; $\sigma_g \rightarrow \pi_u$ $^1P^o$-$^1D^e$; $\pi_u \rightarrow \delta_g$ $^1D^e$-$^1P^o$; $\sigma_g \rightarrow \pi_u$
	n_μ = odd; $\Delta n_\lambda = 1$, $\Delta n_\mu = 1$, $\Delta T = 0$, $\Delta N = \Delta n = 0$	$^1P^o$-$^1D^e$; $\sigma_u \rightarrow \sigma_g$ $^1D^e$-$^1P^o$; $\pi_g \rightarrow \pi_u$ $^1P^0$-$^1S^e$; $\sigma_u \rightarrow \sigma_g$
$\Delta L = 2$	$\Delta n_\lambda = 0$, $\Delta n_\mu = 0$, $\Delta T = 0$, $\Delta N = \Delta n = 0$	$^1S^e$-$^1D^e$; $\sigma_g \rightarrow \sigma_g$

The propensity rules (17) and (18) with $\Delta n_\mu = 0$ show that the doubly excited atom as the "dielectronic molecular ion" tends to keep its internal state the same as that for the initial state. However, the MO model does not give a simple physical interpretation for the propensity rule (19).

For the optically allowed excitation processes with $|\Delta L| = 1$, either one of the propensity rules (14) and (15) has to be modified because of the Pauli exclusion principle for two atomic electrons. The propensity rules (15′) for n_μ even are translated into the following ones, i.e.,

$$\Delta N = \Delta[n_\mu/2] - \Delta n_\lambda + 1, \quad \Delta T = 1 \tag{18′}$$

while for the initial states with $A = -$, i.e., for n_μ odd the propensity rule (14′) is written as

$$\Delta n_\mu = 1 \text{ or odd} . \tag{17′}$$

Again, judging from the smaller overlap of the initial and final wave functions with larger Δn_μ, we may assume $\Delta n_\mu = 1$ for (17′). The propensity rules (18) lead to $\Delta n_\lambda = 1$, $\Delta T = 0$ for $\Delta N = 0$ and so forth. These results are summarized in Table VI, which is the MO version of the propensity rules translated from the rovibrator version given in Table V though the translation cannot be done uniquely.

The propensity rules with $|\Delta L| = 1$ are equivalent to the selection rules of photoabsorption by the atom as pointed out previously. The most important case is the $^1S^e$-$^1P^o$ excitation. For the initial states with n_μ even, we have (17) and (18′) as the propensity rules. This leads to $\Delta n_\lambda = 1$, $\Delta n_\mu = 0$, $\Delta T = 1$ for $\Delta N = 0$. We can rewrite $\Delta T = 1$ in terms of the conventional MO quantum numbers, i.e., $\sigma_g \rightarrow \pi_u$ etc., using relation (9). This is analogous to the selection rule of electronic transition of the diatomic molecule for photoabsorption[21] as is expected.

We have seen that the two models originating from quite different physical pictures can give a reasonable physical interpretation for the propensity rules obtained here in logically consistent manners. This fact is quite interesting and may have a deeper physical meaning for the electron correlation which we have not yet fully understood. Further study is desirable for the elucidation of the correlation effects in collision dynamics involving the doubly excited atoms.

ACKNOWLEDGMENTS

Assistance in the final stage of numerical computation for the $^1P^o$-$^1D^e$ excitation processes by T. Komine is greatly appreciated. This work is partly supported by the Grant-in-Aid for Scientific Research on Priority Areas "Dynamics of Excited Molecules" from the Ministry of Education, Science and Culture of Japan.

*Present address: Fujitsu Limited, 1015 Kami-Odanaka, Nakahara-ku, Kawasaki-shi, Kanagawa Prefecture, 211 Japan.

†Permanent address: All correspondence concerning this article should be sent to M. Matsuzawa at this permanent address.

[1] M. Matsuzawa, T. Motoyama, H. Fukuda, and N. Koyama, Phys. Rev. A **34**, 1793 (1986).

[2] T. Motoyama, N. Koyama, and M. Matsuzawa, Phys. Rev. A **38**, 670 (1988).

[3] M. Matsuzawa, T. Atsumi, and N. Koyama, Phys. Rev. A **41**, 3596 (1990).

[4]C. D. Lin, Adv. At. Mol. Phys. **22**, 77 (1986), and references therein.
[5]N. Koyama, H. Fukuda, T. Motoyama, and M. Matsuzawa, J. Phys. B **19**, L331 (1986).
[6]H. Fukuda, N. Koyama, and M. Matsuzawa, J. Phys. B **20**, 2959 (1987).
[7]N. Koyama, A. Takafuji, and M. Matsuzawa, J. Phys. B **22**, 553 (1989).
[8]D. R. Herrick and M. E. Kellman, Phys. Rev. A **21**, 418 (1980).
[9]M. E. Kellman and D. R. Herrick, Phys. Rev. A **22**, 1536 (1980).
[10]J. M Feagin and J. S. Briggs, Phys. Rev. Lett. **57**, 984 (1986).
[11]J. M. Feagin and J. S. Briggs, Phys. Rev. A **37**, 4599 (1988).
[12]C. D. Lin, Phys. Rev. A **29**, 1019 (1984).
[13]D. R. Herrick and O. Sinanoglu, Phys. Rev. A **11**, 97 (1975).
[14]S. Watanabe and C. D. Lin, Phys. Rev. A **34**, 823 (1986).
[15]J. M. Rost and J. S. Briggs, J. Phys. B **21**, L233 (1988).
[16]J. M. Rost and J. S. Briggs, J. Phys. B **22**, 3587 (1989).
[17]M. Sato, N. Koyama, and M. Matsuzawa (unpublished).
[18]P. J. M. van der Burgt, J. van Eck, and H. G. Heidemman, J. Phys. B **19**, 2015 (1986).
[19]R. P. Madden and K. Codling, Phys. Rev. Lett. **10**, 516 (1963); Astrophys. J. **141**, 364 (1965).
[20]P. R. Woodruff and J. A. Samson, Phys. Rev. A **25**, 848 (1982).
[21]G. Herzberg, *Molecular Spectra and Molecular Structure I, Spectra of Diatomic Molecules,* 2nd ed. (Van Nostrand, Princeton, 1950), p. 243.